Expert Review

Liquid Perfluorocarbons as Contrast Agents for Ultrasonography and ^{19}F-MRI

Raquel Díaz-López,[1,2] Nicolas Tsapis,[1,2] and Elias Fattal[1,2,3]

Abstract. Perfluorocarbons (PFCs) are fluorinated compounds that have been used for many years in clinics mainly as gas/oxygen carriers and for liquid ventilation. Besides this main application, PFCs have also been tested as contrast agents for ultrasonography and magnetic resonance imaging since the end of the 1970s. However, most of the PFCs applied as contrast agents for imaging were gaseous. This class of PFCs has been recently substituted by liquid PFCs as ultrasound contrast agents. Additionally, liquid PFCs are being tested as contrast agents for ^{19}F magnetic resonance imaging (MRI), to yield dual contrast agents for both ultrasonography and ^{19}F MRI. This review focuses on the development and applications of the different contrast agents containing liquid perfluorocarbons for ultrasonography and/ or MRI: large and small size emulsions (i.e. nanoemulsions) and nanocapsules.

KEY WORDS: emulsions; liquid perfluorocarbons; MRI; nanocapsules; nanoemulsions; ultrasonography; ultrasound contrast agents.

INTRODUCTION

Perfluorocarbons (PFCs) are fluorinated aliphatic compounds, wherein all hydrogen atoms in the molecule are replaced by fluorine. The length of the perfluorinated carbon chain determines the perfluorocarbon physical properties. Small chains PFCs, such as perfluoropropane, are gases, and larger chain PFCs, such as perfluorooctane, are liquids denser than water (Fig. 1). They exhibit unique properties (Table I) due to the specificity of the carbon-fluorine linkage that make them attractive for medical purposes. Among these, high oxygen solubility, low surface tension, hydrophobicity and lipophobicity, inertness and absence of metabolism are the most interesting characteristics for their use in clinics (1–3).

Liquid PFCs (Table II) pose minimal toxicological risks compared to gaseous ones (4). Their safety and biocompatibility have been well-documented, mostly pertaining to their development and their use as artificial blood substitutes (5–9),

as well as for liquid ventilation (3,10–12). Only tiny amounts can be systemically given because of their low solubility in water, in biological fats and in lipids, whereas large amounts are administered as a PFC-in-water emulsion. This is the case of perfluoroctylbromide, PFOB ($C_8F_{17}Br$), a liquid PFC which has been used as a potential blood substitute because of its high oxygen solubility, inertness and stability. As PFCs are not miscible with water, an oil-in-water emulsion must be prepared for injection. When such emulsions are used as intravascular oxygen carriers, the elimination half-life of PFOB is 3 to 4 days due to a quick distribution and high tissue retention (13,14). Because PFC molecules are inert to biochemical degradation, they diffuse back into the blood, where they finally dissolve into plasma lipids. These lipids carry perfluorocarbon molecules to the lungs, where they are excreted by exhalation (5,8,9). The main route of elimination of liquid PFCs is exhalation because of their combined hydrophobic and lipophobic character.

Even if liquid PFCs are mostly used as oxygen carriers, they have also been tested as contrast agents for ultrasonography and magnetic resonance imaging (MRI) since the end of the 1970s (4). Indeed, the use of PFCs as contrast agents has been widely discussed, as evidenced by the numerous reviews on the topic (15–20). These previous publications focused mainly on gaseous PFCs, because they have mostly been used as ultrasound contrast agents (UCAs). However, recently, gaseous PFCs contained in UCAs have been substituted by liquid PFCs. Additionally, as novel UCAs based on liquid PFCs were developed, a new application of these agents for magnetic resonance imaging (MRI) has been tested in order to obtain dual contrast agents for both ultrasonography and MRI. This review focuses on the development and applications of the different contrast agent systems based on liquid perfluorocarbons for ultrasonography and/or MRI.

[1] Univ Paris Sud, UMR CNRS 8612, Faculté de Pharmacie, 5 rue Jean-Baptiste Clément, 92296, Châtenay-Malabry, France.

[2] CNRS, UMR 8612, Faculté de Pharmacie, 5 rue Jean-Baptiste Clément, 92296, Châtenay-Malabry, France.

[3] To whom correspondence should be addressed. (e-mail: elias.fattal@u-psud.fr)

ABBREVIATIONS: FDA, food and drug administration; GI, gastrointestinal; i.v., intravenous; MR, magnetic resonance; MRI, magnetic resonance imaging; MRS, magnetic resonance spectroscopy; PEG, polyethylene glycol; PEG-PCL, PEG-*block*-poly(caprolactone); PEG-PLLA, poly(ethylene glycol)-*block*-poly(L-lactide); PFCs, perfluorocarbons; PFD, perfluorodecalin; PFH, perfluorohexane; PFN, perfluorononane; PFOB, perfluorooctylbromide; PFP, perfluoropentane; PLGA, poly(lactide-*co*-glycolide); SNR, signal-to-noise ratio; THI, tissue harmonic imaging; UCAs, ultrasound contrast agents; US, ultrasound.
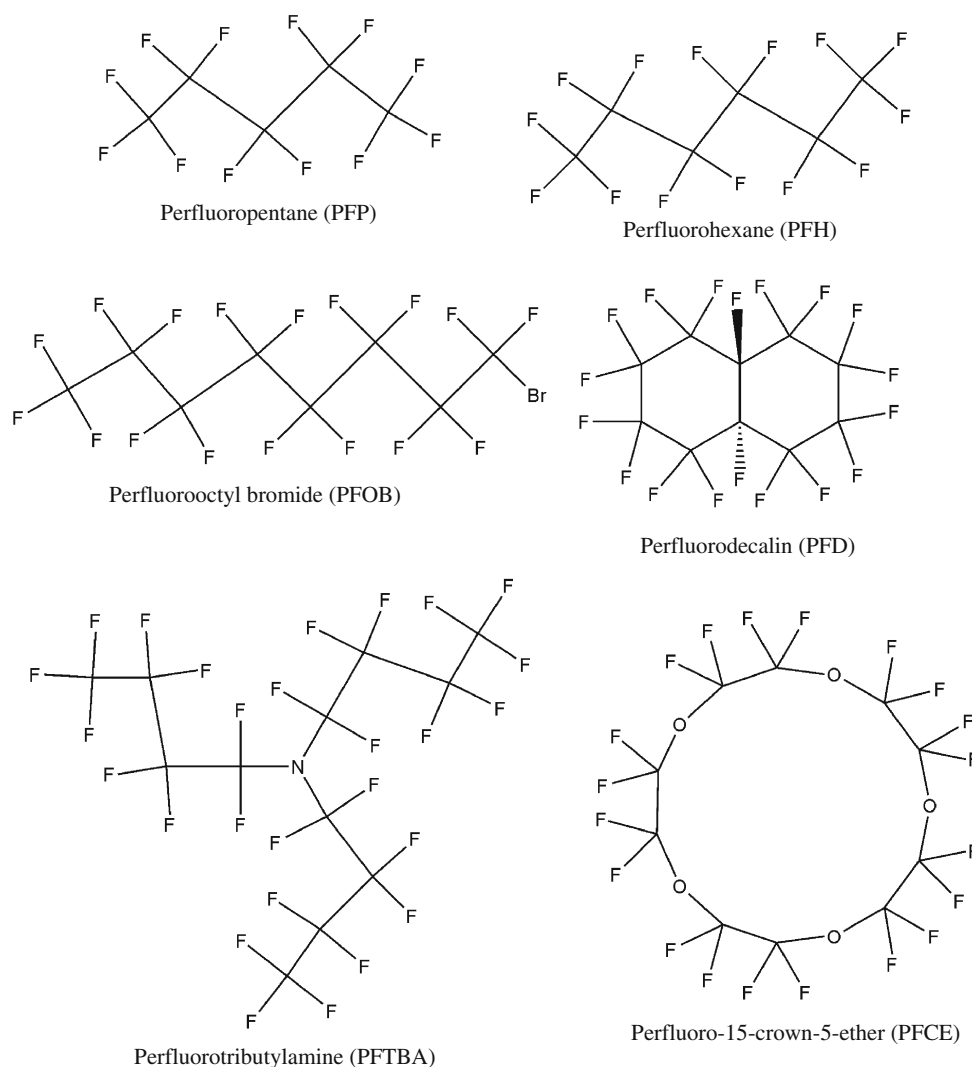
Perfluoropentane (PFP)

Perfluorohexane (PFH)

Perfluorooctyl bromide (PFOB)

Perfluorodecalin (PFD)

Perfluorotributylamine (PFTBA)

Perfluoro-15-crown-5-ether (PFCE)

Fig. 1. Chemical structures of some liquid PFCs.

PRINCIPLE OF ULTRASOUND IMAGING

Ultrasonography, also called ultrasound imaging, is a widely available, non-invasive and cost-effective diagnostic modality that allows the diagnosis of numerous pathological conditions. It uses portable, real-time imaging equipment without requiring hazardous ionizing radiations.

An ultrasound transducer placed on the skin broadcasts ultrasound pressure wave pulses, which are partially back-scattered by interfaces between different tissues or structures in the body. Backscattering occurs because of an impedance mismatch between two different tissues. Impedance is defined as the speed of sound through a material multiplied by the density of the material. Backscattered ultrasound waves return to the transducer and are then converted into electrical pulses by the echograph. Since the time intervals between pulse transmission and reception, as well as the speed of sound in the tissue, are known, an image based on back-scattered sound signals can be generated. The intensity of the backscattered signal from a tissue can be defined as the echogenicity of the tissue. Bones, for example, are very echogenic and therefore can easily be distinguished from soft tissues. Blood vessels, on the other hand, possess a low compressibility; they backscatter ultrasound poorly and are therefore difficult to image (21). Clinical ultrasound frequencies range from 2 MHz to 15 MHz. The higher the frequency, the better the resolution but the lower the depth of ultrasound penentration.

Table I. Properties of Perfluorocarbons

- Fluorinated aliphatic compounds
- Gas or liquid depending of the length of the perfluorinated carbon chain
- Low surface tension
- Low viscosity
- Low diffusion rate
- Low solubility in water, biological fats and lipids
- High gas solubility (O_2 and CO_2)
- High spreading coefficients
- High density
- Stable
- Inert
- Elimination by exhalation

Table II. Physico-chemical Properties of Major Liquid PFCs Used as Contrast Agents

Liquid PFC	Abbreviation	Formula	Molecular weight (g/mol)	Density (g/ml)	Boiling point (°C)
Perfluoropentane	PFP	C_5F_{12}	288	1.62	26–36
Perfluorohexane	PFH	C_6F_{14}	338	1.76	58–60
perfluorodichlorooctane	PFDCO	$C_8F_{16}Cl_2$	471	1.84	115
Perfluorooctyl bromide	PFOB	$C_8F_{17}Br$	499	1.93	140.5
Perfluorononane	PFN	C_9F_{20}	488	1.80	126
Perfluorodecalin	PFD	$C_{10}F_{18}$	462	1.99	144
Perfluoro-15-crown-5-ether	PFCE	$C_{10}F_{20}O_5$	580	1.78	145
Perfluorotributylamine	PFTBA	$C_{12}F_{27}N$	671	1.88	173–181

AIR AND GASEOUS PERFLUOROCARBONS AS CONTRAST AGENTS FOR ULTRASOUND IMAGING

Mechanism of Action of Gaseous Ultrasound Contrast Agents

The weak difference of echogenicity between different soft tissues often hampers a clear diagnostic. For example, the imaging of a breast tumor where the tissue is homogenous requires the use of ultrasound contrast agents (UCAs) to distinguish the tumoral tissue from the healthy one (22). Most of the studies regarding the discovery of new UCAs have focused on the use of air or other biocompatible gaseous ultrasound contrast agents, such as gaseous PFCs.

The principal physical mechanism of gaseous UCAs is the backscattering of ultrasounds from gas microbubbles as they undergo volume oscillations in the sound beam. Due to the high compressibility of gases and their ability to resonate when insonated, a population of microbubbles is very effective in backscattering incident ultrasounds as compared with surrounding blood or tissue (21,23). The acoustic back-scattering arising from microbubbles is greater than the backscattering arising from the blood and the majority of other tissues and organs. This is due to the high acoustic impedance mismatch between gases and blood or soft tissue. During ultrasound scanning, body cavities and compartments containing microbubbles will appear white as compared with regions devoided of contrast agents (24).

The microbubble acoustic backscattered signal depends on the gas compressibility, the microbubble size and shell thickness, the viscosity and density of the microbubble shell, the properties of the surrounding medium, and the frequency and power of the applied ultrasounds (25). The backscattered signal is proportional to the concentration of the contrast agent present at a given site. The resonating ability of microbubbles is of the utmost importance since it can produce up to three orders of magnitude more signal than plain backscattering (26). The size of microbubbles also is an important parameter to control, because the larger the microbubbles, the more echogenic. However, a size compromise must be found since the largest particle able to transit via normal pulmonary and systemic capillary beds should not exceed 6 μm to 8 μm in diameter. Furthermore, one must take into account that microbubble size may change after injection because of potential bubble coalescence, gas core expansion or contraction, and inward/outward diffusion of gases, depending on the temperature, vapor pressure, hydrostatic pressure, acoustic pressure (17).

Properties of Ideal Gaseous Ultrasound Contrast Agents

Since UCAs are administrated by perfusion or by an intravenous (i.v.) injection, their size is an important parameter to control. A successful contrast agent must be injected easily through a peripheral vein and have the ability to pass unimpeded through the pulmonary circulation. Passage through the lungs is necessary for the agent to remain intact in the blood stream for an extended period of time to allow adequate scanning of the organ of interest (27). Since the average diameter of lung capillaries is between 4 μm to 7 μm, in order to avoid potential capillary embolism, the size of UCAs should be smaller than approximately 4 μm (28). UCAs' diameters should be well-controlled and should not increase after injection. Additionally, a contrast agent also has to be highly compressible and to backscatter ultrasound waves several orders of magnitude more effectively than red blood cells. It should also demonstrate long circulatory persistence to ultrasonic destruction while displaying significant echogenicity to give sufficient time for imaging. Its components need to be safe and readily excretable (1). Nevertheless, although ideal, these properties do not exclude some important drawbacks that limit the use of gaseous UCAs.

Drawbacks of Air or Gaseous Perfluorocarbons as Ultrasound Contrast Agents

One of the main drawbacks of air-based UCAs is that they do not allow observing contrast into organs other than the left heart chamber after an i.v. injection; two commercial UCAs—Levovist® (air bubbles stabilized by palmitic acid), a registered trademark of Schering AG, and Albunex® (air bubbles stabilized by albumin) of Mallinckrodt Inc.—exhibit this drawback. The principal explanation is that these UCAs are too large to pass unimpeded through the pulmonary capillaries. Additionally, as air is highly soluble in the blood and diffuses easily, microbubbles simply deflate quickly after injection as air dissolves into the blood (23,28). Moreover, microbubbles are susceptible to destruction by ultrasounds. In an effort to increase the stability of UCAs, air was replaced by gaseous PFCs whose solubility in blood is lower and which diffuse more slowly. Encapsulation of gaseous PFCs improves stability against gas loss, dissolution, and microbubble coalescence, and produces a more standard size distribution. A surfactant layer increases the half-life of the microbubble by decreasing surface tension (21). The gaseous PFCs formula-

tions were effective for blood pool opacification, but their overall efficacy is diminished by particle instability to insonification pressures, marked attenuation, "blooming" effects and short circulation times (28,29). Most recent commercial UCAs consist of gaseous perfluorocarbon bubbles stabilized either by polymer or lipid shells. SonoVue™ of Bracco is composed of sulphur-hexafloride stabilized by phospholipids (30). Definity® of Bristol-Myers Squibb contains perfluoropropane stabilized by phospholipids (31,32). Optison™ of GE Healthcare (33) consists of microbubbles of perfluoropropane stabilized by albumin. The combination of a perfluorinated gas, displaying a low diffusion coefficient and low solubility in blood and surrounded by a biodegradable and non-toxic polymer, allows for an increase of the plasmatic half-life of UCAs (>5 min), in comparison with traditional air microbubbles (15,21,25).

In conclusion, commercial UCAs consisting of encapsulated gas microbubbles injected intravenously improve visualization of the vascular tree, but their limited stability hampers their use as molecularly targeted agents (34). Stabilization of microbubbles by polymers increases the stability of UCAs, since polymeric shells resist dissolution and acoustic pressures better than the monomolecular layers of lipids or proteins usually stabilizing commercial UCAs (35–37). Moreover, because of their high difference of density with air and their poor solubility in water, gaseous perfluorocarbons have been shown to increase both the stability and the echogenicity of UCAs (38). Nevertheless, the circulation time of such gaseous UCAs is still very short to allow their distribution into poorly accessible body sites, such as tumoral or inflammatory sites.

LIQUID PERFLUORCARBONS AS ULTRASOUND CONTRAST AGENTS

Recently, liquid PFCs have been used instead of gaseous PFCs because they lead to UCAs that are more resistant to pressure changes and mechanical stresses. The use of liquid PFCs as contrast agents—perfluoroctylbromide, PFOB ($C_8F_{17}Br$), in particular—was considered since the mid 70's. In 1977, Liu and Long (4) were the first to report the efficacy and safety of PFOB as a diagnostic contrast medium for gastroenterography after an oral administration in different animal models. The stomach and small intestine were well-defined with a good separation of the small bowel. However, to make liquid PFC able to be administered by the parenteral route, particulate systems were designed consisting of a lipidic layer surrounding PFC droplets for emulsion (large or small size, i.e., nanoemulsions) or a polymeric shell encapsulating PFC in the case of nanocapsules (Fig. 2).

Large Size Perfluorocarbon Emulsions

Very early, emulsions were designed to disperse PFOB in an aqueous injectable solution. In 1982, Mattrey *et al.* (39) showed that PFOB emulsions stabilized by pluronic F-68, with droplet size smaller than 0.5 μm, caused a delayed and persistent enhancement of the ultrasound signal in rabbit liver 48 h after an i.v. injection as a result of an accumulation of PFOB within the Kupffer cells. Computed tomography and chemical analysis have proved that PFOB emulsions accumulate in the spleen as well as in the liver and in rabbit hepatic
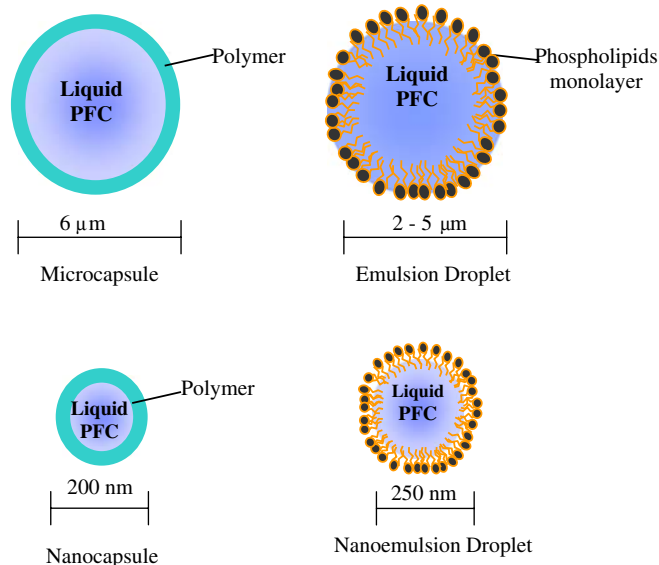

Fig. 2. Scheme of systems of contrast agent with liquid PFCs.

tumors (13,14). PFOB emulsions appeared to have an excellent potential for imaging the mononuclear phagocyte system and for the opacification of blood vessels for prolonged periods of time. Although these results were promising, it was necessary to wait until 1994 before Sonus Pharmaceuticals® began the development of a new contrast agent with a liquid PFC, called EchoGen®. EchoGen® is an emulsion of perfluoropentane (PFP) that is liquid at room temperature and undergoes a liquid-gas phase transition at body temperature because of a low boiling point (28°C). It is supplied as an aqueous emulsion in 30% sucrose at 2% perfluoropentane for intravenous injection. Surfactants used to stabilize EchoGen® were not specified. Once in the circulation, the PFP droplets contained in the emulsion turned into microbubbles. Microbubbles were around 2–5 microns in size. Some of them were small enough to pass the lung capillaries. Perfluoropentane was totally excreted through the normal breathing process (40). EchoGen® was able to produce the opacification of the left ventricule and myoacardium during 20 s following i.v. injection at very low doses: 0.05 mL/kg to 0.1 mL/kg in cats. Using higher doses (0.4 ml/kg to 0.8 ml/kg), opacification persisted up to 35–40 min (41,42). When given intravenously to normal human volunteers, EchoGen® emulsion provided qualitative information about the perfusion of the myocardium without inducing any side effects (43). The persistence of the contrast effect allows the visualization of the cardiac muscle from different points of view. Using the PFC emulsion, it was possible to apply echocardiography to visualize myocardial perfusion deficits by producing a negative contrast effect, giving the possibility to physicians to diagnose coronary artery diseases (44). EchoGen® has also been used as a contrast agent to improve the visualization of blood-flow in the prostate, allowing for better imaging of prostate microcirculation and improving the detection of prostate cancer (40). EchoGen® passed phase I and II of clinical trials, and in 1998 its commercialization in Europe was approved. However, in 2000, the product was withdrawn from the market by Sonus Pharmaceuticals® supposedly because Sonus decided

to stop marketing contrast agents to refocus on the development of its drug delivery and blood substitute products.

Nevertheless, several research groups pursued their studies on the use of PFC emulsions. Indeed, in order to consider the application of PFC emulsion for molecular imaging of atherosclerosis, an inflammatory disease of arteries, Kornmann *et al.* (45) investigated their uptake by macrophages derived from bone marrow. Macrophages were chosen as a targeted vehicle for UCAs because they play a crucial role in the development of atherosclerosis (46). They are indeed involved in all stages of atherosclerotic plaque development and are increasingly perceived as candidates for therapeutic intervention and potential biomarkers of disease progression and response to therapy. It was important to understand whether these cells show sufficient echogenicity to be detected by ultrasound maintaining their adhesive properties. Emulsions were composed of perfluorohexane (PFH) droplets of about 1 micron stabilized by a mixture of phospholipids. The study demonstrates that at least in an *in vitro* setting, PFH emulsions loaded within macrophages did not lose their echogenic property and that cells maintained their adhesive properties for 24 h. Macrophages internalizing PFC emulsions exhibited a strong dose-dependent increase in echogenicity up to a maximum for 4% emulsion loading.

Small Size Perfluorcarbons Emulsions or Nanoemulsions

All emulsions described before had a diameter much larger than 1 μm. Although they have been used with varying degrees of success, there are still some difficulties associated with their size. When injected intravenously, UCAs of large size generally around 4–5 μm remained trapped in pulmonary capillaries and could not pass from the right side to the left side of the heart. By contrast, it is believed that smaller UCAs remain in the vasculature as long as they are not recognized and cleared by the immune system. Indeed, due to the uptake by macrophages of the mononuclear phagocyte system, the half-life of UCAs has been shown to be very short (<5 min) (15,25).

Nanosystems based on liquid PFC of about one to two hundreds of nanometers, approximately ten-fold smaller than commercially available microbubble contrast agents, offer the potential for extravascular diagnosis. If designed properly, they can escape macrophage uptake (47) and even undergo an enhanced permeability and retention effect (48) in neovascularized tumors, provided their surface is covered by hydrophilic poly(ethylene glycol) polymers (49,50) (Fig. 3). Molecular imaging might also be considered, provided nanosystems possess at their surface ligands for particular receptors. These advantages of nanosystems have been taken into account by researchers in their development of nanometric UCAs based on liquid PFCs using lipids as stabilizing amphiphilic molecules leading to the formation of nanoemulsions (Table III).

The group of Lanza and Wickline has shown that nanoemulsions of liquid perfluorocarbons in water have interesting echogenic properties (51). Indeed, they have designed a site-specific UCA for non-invasive detection of vascular thrombi using a clinical frequency (7.5 MHz). This UCA is designed to specifically and sensitively enhance the acoustic reflectivity of a pathological tissue that would otherwise be difficult to distinguish from surrounding normal

tissue. It consists of a biotinylated, lipid-coated, nanoemulsion of liquid perfluorodichlorooctane (PFDCO), whose size is around 250 nm. The nanoemulsion is administered by a three-step approach. In the first step, biotinylated antifibrin monoclonal antibodies are administered intravenously. They binds to the target. In a second step, avidin, which conjugates and cross-links the biotinylated ligand, is given, increasing the "avidity" of the complex for the tissue surface. In a third step, the biotinylated emulsion is administered and attaches to the bound antibody-avidin complexes through unoccupied biotin receptor sites. Although circulating droplets had a poor acoustic reflectivity, the aggregated particles markedly increased the acoustic reflectivity at the targeted site. The acoustic contrast effects of the biotinylated and control nano-emulsions before and after exposure to avidin were measured within dialysis tubes. Before the addition of avidin, neither the control nor the biotinylated emulsion had significant acoustic reflectivity. Addition of avidin had no effect on the echogenicity of the control perfluorocarbon emulsion. The biotinylated perfluorocarbon emulsion displayed a rapid increase in acoustic reflectivity up to 30 min after the addition of avidin. The same biotinylated nanoemulsions were also applied to target the tissue factor (52). Tissue factor is a glycoprotein that plays important roles in angiogenesis and tumor cell metastasis. It has been used as a target for destroying tumors *in vivo*. Using the biotinylated nanoemulsions, Lanza *et al.* (52) succeeded to visualize the stretch of pig carotid arteries induced by tissue factor. They demonstrated *in vivo* molecular imaging of intra-arterial tissue factor expression, which reflects the injury of the arterial wall of carotids.

In following studies, perfluorodichlorooctane was sub-stituted by perfluoroctylbromide (PFOB) most probably for toxicity reasons as reported by Winslow (53) or because the PFDCO manufacturer (3M and Hemagen) decided to dis-continue PFDCO use for medical applications. The efficacy of PFOB nanoemulsions as a blood pool contrast agent for the assessment of ventricular function and wall motion abnormal-ities was demonstrated using Power Doppler Harmonic Imaging (28,29). Two nanoemulsions of different diameters, 232 nm and 465 nm, were formulated. *In vivo* imaging was performed after i.v. injection in a canine model at a dose of 0.5 ml/kg. Only for the larger droplets, a marked enhance-ment and delineation of the left ventricular blood pool and endocardial borders were produced, and contrast persisted during 1 h. The acoustic contrast effect depended on nano-emulsion size but was unaffected by continuous ultrasonic imaging and was effective at low dosage (0.7% blood volume). In conclusion, although PFOB nanoemulsions exhibited long circulatory times and were stable to insonifi-cation, they yielded a poor echogenicity (28).

In addition to their large body of experiments, Lanza and coworkers have also developed theoretical models to estimate the acoustic reflectivity of nanoemulsion formulations prepared with different liquid PFC and also to quantify the relationship between the contrast enhancement of targeted surfaces and the concentration of nanodroplets (54–57). These models using highly sensitive entropy detection algorithms were successfully applied for detection of tumor neovasculature *in vivo* to differentiate between targeted and untargeted vessels (58–60). According to the authors, these algorithms could be easily implemented on any ultrasound machine, even without using
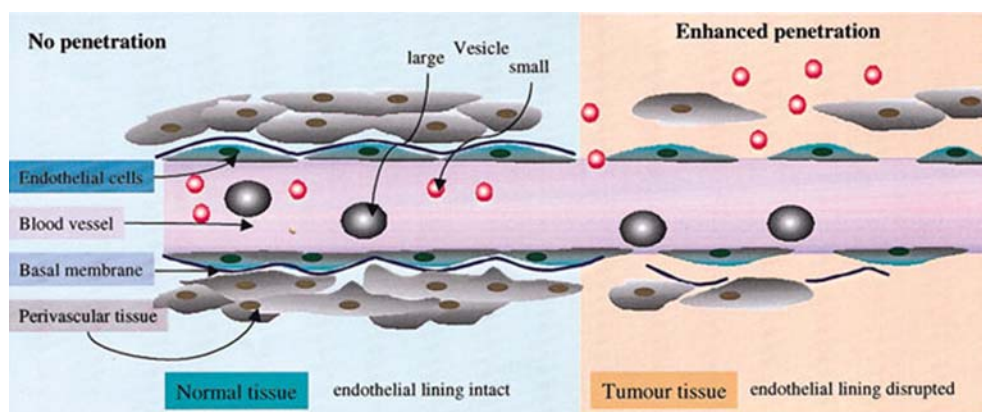
Fig. 3. Accumulation of liposomes within solid tumours, (*right*) nanoparticle extravasation from the disorganised tumour vasculature and (*left*) nanoparticle in normal tissue (76). Reprinted with permission.

PFCs. Models were also revisited by Couture *et al.* (61,62) showing that the reflectivity of PFC nanoemulsions is enhanced once droplets are bound onto a surface.

Polymeric UCAs Containing Liquid PFC

Polymers were first used to increase the stability of microbubble-based UCAs since polymeric shells are much more resistant to ultrasonic waves than monomolecular layers of lipids or surfactants (15,25,35,36,63). To combine the chemical versatility of polymers with the imaging advantages of liquid perfluorocarbons, their encapsulation within polymer nanocapsules has been considered. Pisani *et al.* (64–66) have designed a process, based on a modified solvent emulsion/evaporation method, to obtain nano/microcapsules with a single core of liquid PFC within a polymer shell of homogeneous thickness. The process has been optimized with poly(lactide-co-glycolide) (PLGA), the most common biodegradable (67) and biocompatible polymer (68). Several PFCs were tested with boiling points ranging from 36°C for perfluoropentane to 140°C for PFOB.

Microcapsules could be obtained with PFOB, perfluorodecalin (PFD) and perfluorohexane (PFH) but not with perfluoropentane (PFP). The failure of PFP encapsulation probably arises from the low boiling point of this chemical, close to the boiling point of methylene chloride, the solvent used for capsule preparation. The method of preparation allows the mean capsule diameter to be regulated between 70 nm and 25 μm (Fig. 4). In addition, the thickness-to-radius ratio of the shell (T/R) can be adjusted between 0.25 and 0.54 for PFOB simply by modifying the polymer-to-PFOB ratio in the organic phase prior to emulsification (64). Capsule diameter remained stable at 37°C in phosphate buffer for at least 4 h and 6 h for nanocapsules and microcapsules, respectively. The *in vitro* ultrasound signal-to-noise ratio (*SNR*) was measured from 40–60 MHz for 6 μm and 150 nm capsules: the *SNR* increased with capsule concentration up to 20–25 mg/ml, and then reached a plateau that depended on capsule diameter (13.5±1.5 dB for 6 μm and 6 dB±2 dB for the 150 nm capsules). The ultrasound *SNR* was stable for up to 20 min for microcapsules and for several hours for nanocapsules. For nanocapsules, the thinner

Table III. Summary of Systems with Liquid PFC Used as UCAs

| System developed	Liquid PFC used	Goals	Echographic evaluations	Reference
Emulsion	PFH	Molecular imaging of atherosclerosis by the capture of macrophages	*In vitro* echogenicity	(45)
Nanoemulsions	PFOB	Blood pool UCA for the ventricular function and wall motion abnormalities	*In vitro* and *in vivo* imaging on canine model	(28, 29)
	PFH	Drug delivery carriers for camptothecin, active acoustically	*In vitro* ultrasonic effect on drug release	(72)
Biotinylated nanoemulsions	PFDCO	Site-specific UCA for noninvasive diagnosis of vascular thrombi	*In vitro* and *in vivo* imaging on porcine clots and canine model	(51)
	PFDCO	Targeted agent for molecular imaging of tissue factor within carotid arteries	*In vivo* imaging on pig model	(52)
Pegylated polymeric microcapsules	PFOB	Blood pool contrast and hepatic imaging	*In vitro* echogenicity	(71)
Polymeric micro/nanocapsules	PFOB	Blood pool contrast and hepatic imaging	*In vitro* and *in vivo* imaging on mouse model	(65)
Polymeric nanoparticles to nano/microbubbles	PFP	Tumor imaging and targeted chemotherapy with doxorubicin	*In vitro* cavitation activity and *in vivo* tumor imaging on mice Ultrasound-triggered drug release	(73,74)
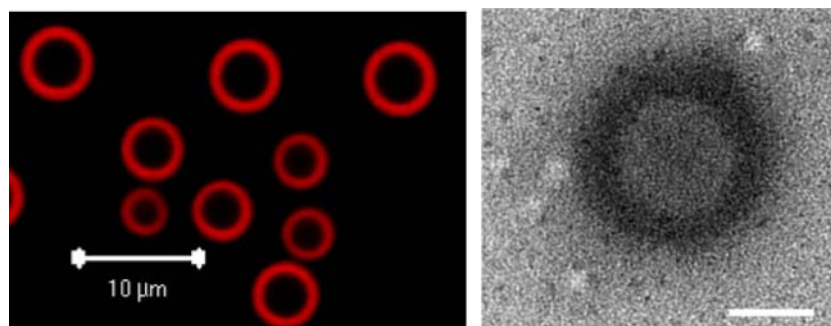
Fig. 4. Confocal microscopy image (scale bar = 10 μm). PLGA is dyed in red, whereas PFC appears *dark* (*left*). TEM image of a typical nanocapsule: because of the difference of electronic density, the PFOB liquid core appears in *gray*, whereas the polymeric shell seems darker; the scale bar represents 100 nm (*right*) (64). Reprinted with permission.

the shell, the larger the *SNR* and the more compressible the capsules. Nanocapsule suspensions imaged *in vitro* with a commercial ultrasound imaging system (normal and Tissue Harmonic Imaging modes, 7–14 MHz probe) were detected down to concentrations of 12.5 mg/ml. Injections of nanocapsules (200 μL at 50 mg/ml) in mice *in vivo* revealed that the initial bolus passage presents significant ultrasound enhancement of the blood pool during hepatic imaging (7–14 MHz probe, Tissue Harmonic Imaging mode) (65). However, the inferior vena cava was enhanced only for a few seconds after injection (Fig. 5). The enhancement disappearance may have resulted from the rapid dilution of the bolus in the total blood volume, leading to a final concentration of approximately 2 mg/mL, which is well below concentrations detected *in vitro*. The concentration of the capsules in circulation would be further reduced as a function of time due to uptake by macrophages of the mononuclear phagocyte system, since the injected capsules were designed to escape this mechanism of clearance (34,47).

In a strategy to increase the circulation time of the nanocapsules and take advantage of the enhanced permeation and retention effect to passively target tumors, PEGylation of capsule surface has been considered. By its hydrophilic nature, PEG provides protection from blood proteins adsorption, and uptake by the mononuclear phagocyte system is drastically reduced (69). Furthermore, PEG is non-toxic, safe and has a good biocompatibility (70). Diaz-Lopez *et al.* (71) modified microcapsules obtained by Pisani, incorporating PEGylated phospholipids in the organic phase prior to emulsification. Phospholipid chains preferentially distribute into the hydrophobic PLGA matrix, whereas their hydrophilic head groups (PEG) are oriented towards the hydrophilic external environment as confirmed by confocal microscopy and X-ray photon spectroscopy. PEGylation did not modify the *in vitro* echographic signal arising from microcapsules. The feasibility of capsule functionalization was also proved using biotinylated PEGylated phospholipids (71). The very same strategy was applied successfully to PEGylation of PFOB nanocapsules (Diaz-Lopez *et al.* in preparation).

Drug Loading Within PFC-Containing Contrast Agents and Ultrasound-Triggered Release

Another interesting feature of PFC nanoemulsions is their capacity to carry a therapeutic payload. Since nanoemulsions can be targeted to specific tissues, they may help increase the local drug concentration in a desired tissue while minimizing the deleterious effects on healthy tissues. In addition, ultrasounds can also be used to trigger drug release in the target tissue. Fang *et al.* (72) developed acoustically active nanoemulsions containing camptothecin, a potent anticancer agent active against a broad spectrum of cancers.
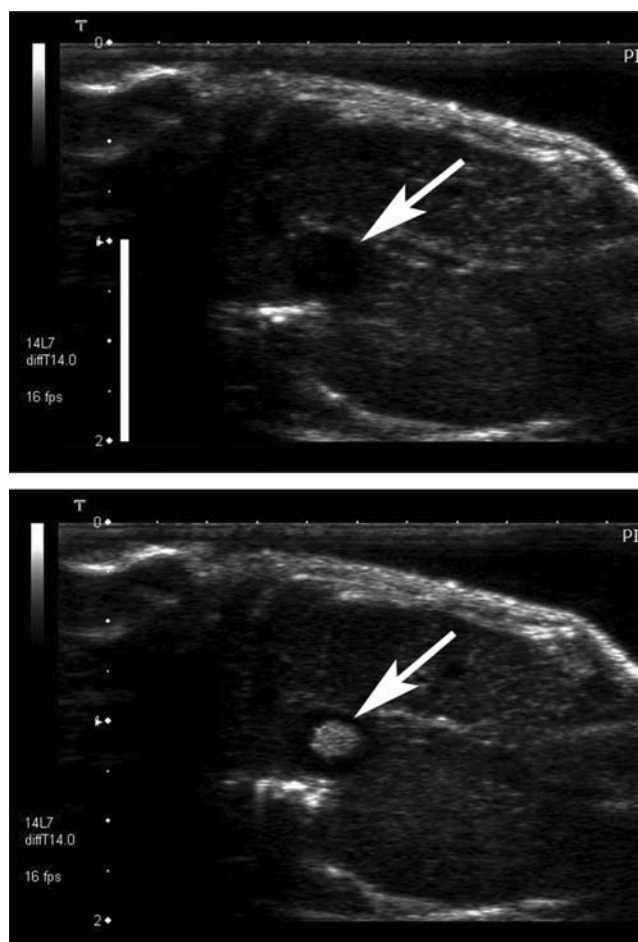

Fig. 5. Ultrasound images of mouse liver obtained in THI mode before (*top*) and after a 200 μL injection of a 50 mg/ml suspension of 150 nm diameter capsules. The inferior vena cava (noted by an *arrow*) appears *dark* in the center of the top image, and presents significant enhancement after capsule injection (*bottom*). The scale bar represents 1 cm. (65) Reprinted with permission.
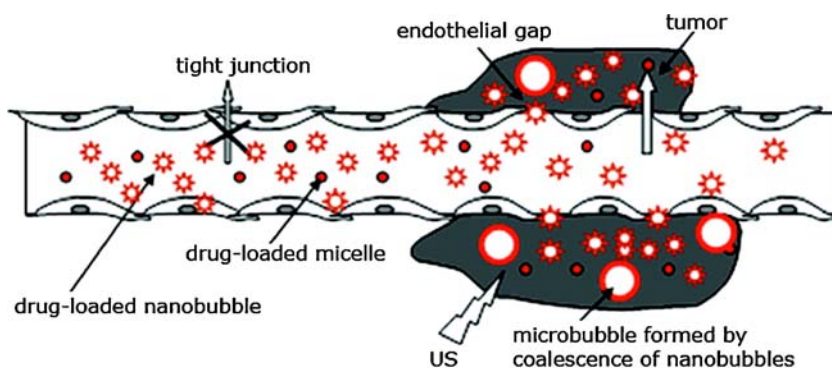
Fig. 6. Schematic representation of drug targeting through the defective tumor micro-vasculature using the echogenic drug delivery system. The system comprises polymeric micelles (*small circles*), nanobubbles (*stars*), and microbubbles (*large circles*), Rapoport *et al.* (73). The tight junctions between cells in endothelial lining of the blood vessels in normal tissues do not allow extravasation of drug-loaded micelles or nano/microbubbles (indicated by *cross*). In contrast, tumors are characterized by defective vasculature with large gaps between the endothelial cells, which allows extravasation of drug-loaded micelles and small nanobubbles resulting in their accumulation in the tumor interstitium. On accumulation in the tumor tissue, small nanobubbles coalesce into larger, highly echogenic microbubbles. Reprinted with permission.

Nanoemulsions were prepared using mixtures of perfluoro-hexane and coconut oil as the core of the emulsions and phospholipids and/or pluronic F68 as stabilizers. The mean droplet diameter was between 220−420 nm, and the drug loading was around 0.05%. Ultrasounds were effective to increase drug release form the nanoemulsions. As for nano-emulsions, nanocapsules may also be loaded with lipophilic drugs for drug delivery purposes. Rapoport and Gao (73,74) developed multifunctional nanoparticles to combine ultra-sonic tumor imaging and targeted chemotherapy, using perfluoropentane (PFP) as liquid PFC. Mixtures of drug-loaded polymeric micelles and PFP nanoparticles stabilized by the same biodegradable block copolymer were prepared. Polymeric nanoparticles were formed by self-assembly of amphiphilic block copolymers: poly(ethylene glycol)-*block*-poly(L-lactide) (PEG-PLLA) or PEG-*block*-poly(caprolac-tone) (PEG-PCL). Doxorubicin, a lipophilic drug, is localized in the micelle core and in the walls of nano/microbubbles. Indeed, at physiological temperatures, nanoparticles are con-verted into nano/microbububles, because PFP boiling point is 28°C. Upon intravenous injection to mice, doxorubicin-loaded micelles and nanobubbles accumulated selectively into the tumor interstitium thanks to the EPR effect (75,76) (Fig. 6). In the tumor tissue, small nanobubbles coalesced into larger, highly echogenic microbubbles (Fig. 7). Tumor-accumulated micobubbles provided a long-lasting ultrasound contrast (Fig. 8) and also allowed local release of the encapsulated drug triggered by ultrasounds. Doxorubicin was then taken up by tumor cells *in vitro* and resulted in tumor regression in the mouse model (73,74).

LIQUID PFC FOR MRI

Besides their echogenic properties, liquid perfluorocar-bons also have applications with another non-invasive imag-ing technique: magnetic resonance imaging (MRI). MRI is a diagnostic scanning technique based on the principle of nuclear magnetic resonance. The term "nuclear" has long been dropped from the description of medical MR techniques because of its association with radiation and radioactivity. This technique does not use radioactivity or X-rays and provides high-resolution tomographic images with an excel-lent soft tissue contrast and versatile functional capabilities. Consequently, using this technique, it is possible to obtain very accurate anatomical localization of a molecular signal, which is important for diagnosis (77). Unlike ultrasonogra-phy, where the resulting image is based primarily upon the differential attenuation of adjacent structures, there are many more factors that contribute to the final appearance of the image in MRI.

Principle of MRI

Conventional ^{1}H-MRI is based upon the property of hydrogen nuclei to align with and precess around an applied static magnetic field. The precessing hydrogen nuclei can be perturbed by radio frequency pulses, and the processes through which they return to their original aligned state can be exploited to give an image. The contrast comes from local differences in spin relaxation kinetics along the longitudinal (spin−lattice relaxation time T_1) and transverse (spin−spin relaxation time T_2) planes of the main magnetic field applied. All tissues have different T_1 and T_2 relaxation times based on their proton/water content. By varying the time to detect the signal (TE—time to echo) and the time to apply the next radiofrequency pulse (TR—time to repetition), one can optimize the signal (78).

MRI Contrast Agents

As for ultrasonography, ^{1}H-MRI contrast agents enhance the image contrast between normal and diseased tissue and can indicate the status of organ function or blood flow after administration by modifying the relaxation rates of protons in tissue in which the agent accumulates (79). Two classes of contrast agents exist: T_1-contrast agents, which lead to positive contrast enhancement, providing a brighter signal where they accumulate, or T_2-contrast agents, which lead to
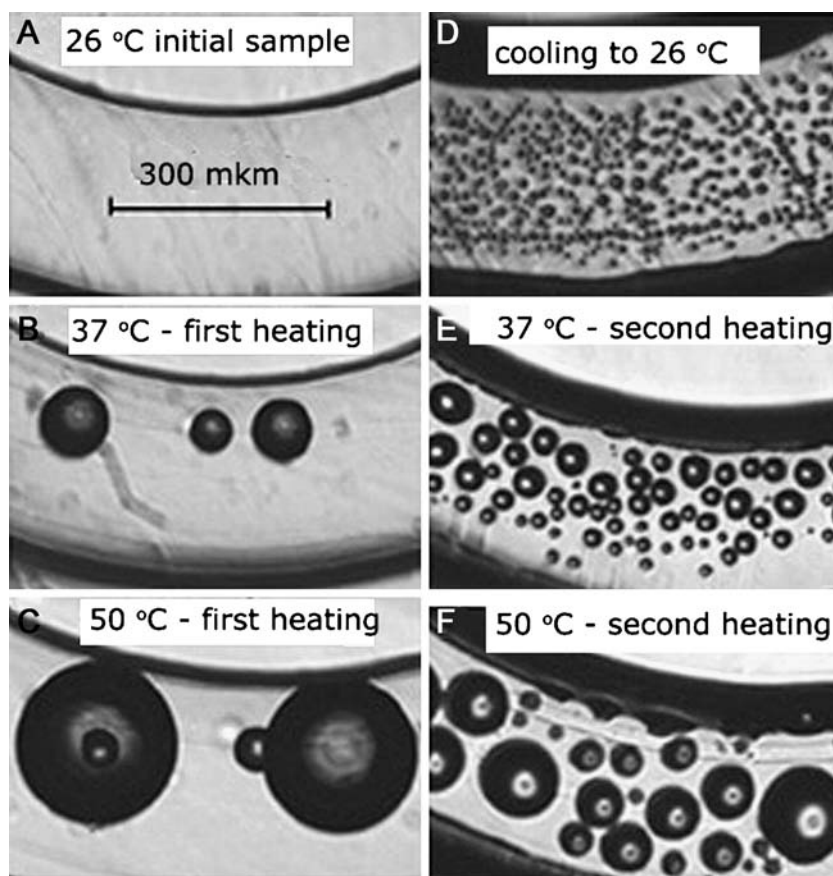
Fig. 7. Optical images of a PEG-PLLA/perfluoropentane formulation placed in a closed plastic capillary (internal diameter 340 mm) of a snake mixer slide. The sample was visualized during a heating/cooling/heating cycle using a heating stage and a fluorescence microscope. **A**) At 26°C, nanoparticles of PEG-PLLA/ PFP were not resolved at the highest available magnification (×100). **B** and **C**) Upon heating to 37°C (**B**) and 50°C (**C**), large bubbles grew by attracting and coalescing with small ones. **D**) After the sample was cooled back to room temperature, the initial structure was not restored, and a large number of small microbubbles were formed. **E** and **F**) Images were taken during a second heating step at 37°C and 50°C, respectively; growth of large microbubbles via the attraction and coalescence with small ones was manifested by a progressive decrease in the number of small microbubbles, Rapoporte *et al.* (73). Reprinted with permission.

negative contrast enhancement, providing darker signal where they accumulate. Gadolinium-diethylenetriaminepentaacetate chelates (Gd-DTPA) are typical T1-contrast agents, whereas Superparamagnetic Iron Oxides (SPIOs) or Ultrasmall Superparamagnetic Iron Oxide (USPIOs) are typical T2-contrast agents (80).

^{19}F-MRI

Although ^{1}H-MRI is most frequently performed, ^{19}F MRI presents several advantages. Fluorine is an excellent element for MRI because ^{19}F has the following characteristics: (1) a gyromagnetic ratio close to that of ^{1}H; (2) a spin ½ nucleus; (3) a 100% natural abundance; (4) a relative sensitivity corresponding to 83% of ^{1}H; (5) no detectable background concentration; (6) a larger outer-shell of electrons (7 *vs* the 1 for hydrogen) (81). Moreover, the fluorine present in the body is mostly in the form of solid fluoride in bones and teeth, and since endogenous fluorine has a very short T_2 relaxation time, the resulting signal is below the limits of MRI detection in most biological systems. The absence of naturally occuring fluorine in biological tissue has two advantages. First, it enables imaging of very small amounts of exogenous fluorinated compounds, since there are no competing signals in the body. Second, as the signal is derived only from the fluorinated compound, it will be much less complex than, for example, a proton signal where a multiplicity of components with different relaxation times could be present (81,82).

In spite of these advantages, several technical problems associated with fluorinated compounds have inhibited the widespread use of ^{19}F MRI *in vivo*. Indeed, they present relatively long T_1 and short T_2 relaxation times, resulting in long image acquisition times and MR signal attenuation, respectively. In addition, the wide-range distributed chemical shifts of ^{19}F NMR signals tend to give rise to chemical shift artifacts in the MR image, although these chemical shifts can be used to trace the metabolism (83). However, using high fluorine concentrations, such as those accessible with PFCs, the signal-to-noise ratio will be enhanced and the scanning time decreased for high-resolution images aquisition.
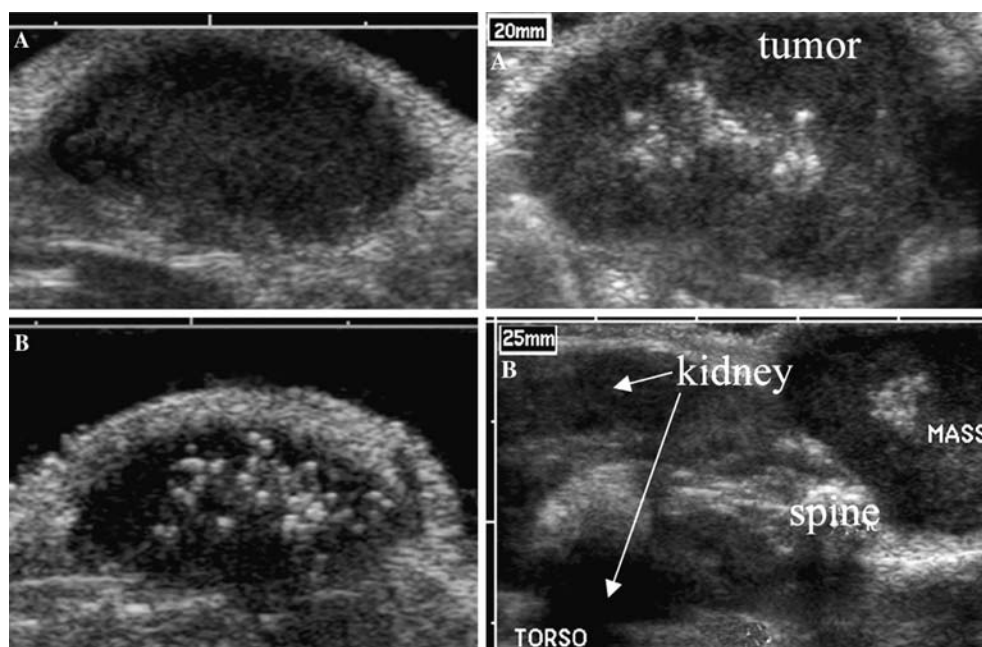
Fig. 8. B-Mode ultrasound images of MDA MB231 human breast cancer-bearing nude mouse of 100 μl 0.5% PEG-PLLA/2% PFP formulation. *Top*, images (**A**) before the intra-tumoral contrast injection and (**B**) 4 h after the intratumoral injection. Bottom images, following intravenous contrast injection: (**A**) tumor image taken 4.5 h after the intravenous (**B**) *trans*-torso image of the same mouse showing a tumor (designated as "mass"), kidneys, and spine. The images show that echogenic microbubbles were accumulated in the tumor but not in the kidney. Images were taken using a 14-MHz linear Acuson Sequoia 512 transducer. Strong ultrasound contrast in the tumor persisted for several days (73). Reprinted with permission.

Liquid PFC as Contrast Agents for ^{19}F-MRI

Due to the lack of ^{19}F endogenous background signal *in vivo* and to its high MR sensitivity, liquid PFC could represent ideal agents for magnetic resonance imaging. For instance, the literature shows that liquid perfluorononane (PFN) directly administered orally to mice (84) can be monitored through the entire gastrointestinal (GI) tract by repetitive MR measurements. In this experiment, high-resolution images of the GI wall were obtained (Fig. 9). Although PFN had to be administered in rather large quantities to delineate the entire GI tract, it appeared to be well-tolerated (84). As for ultrasound contrast agents, the use of liquid dispersions has allowed the parenteral administration of PFC. Liquid PFCs have been encapsulated either within a lipidic or a polymeric shell as ^{19}F-MRI contrast agents (Table IV).

PFC Emulsions

Liquid PFC emulsions were first used as intravascular oxygen carriers to improve oxygen delivery in biological systems because of their unique capacity for transport of
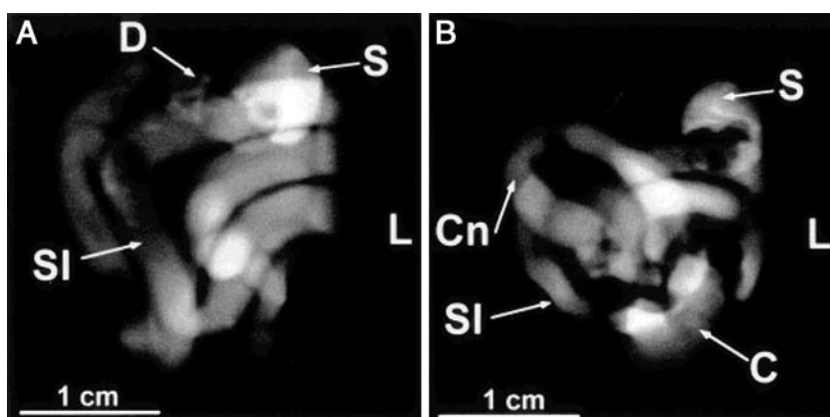

Fig. 9. ^{19}F-MR images of the gastrointestinal tract of a mouse obtained after successive gavages of 0.3 ml of perfluorononane administered every 30 min over a period of 2.5 h. (**A**) Acquired immediately after the last gavage; (**B**) obtained after a wake-up period of 1 h. *L*, left-hand side; *S*, stomach; *D*, duodenum; *SI*, small intestine; *C*, cecum; *Cn*, colon (84). Reprinted with permission.

Table IV. Summary of Systems Developed with Liquid PFC for ^{19}F-MRI

System developed	Liquid PFC used	Objective of the system	Evaluations done	Reference
Nanoemulsion	PFCE	MRI of inflammatory processes	*In vivo* MRI on mice	(107)
	PFOB or PFCE	MRI of mononuclear, stem/progenitor cells for their tracking	MR Spectroscopy, MRI of *in situ* cells and *in vivo* in mice	(100,101)
	PFCE	MRI for tracking dendritic cells	*Ex vivo and in vivo* MRI on mice	(104)
Nanoemulsion with gadolinium compound	PFCE	Cardiovascular MR angiography	MR *In vitro and in vivo* MRI on mice	(99)
Biotinylated nanoemulsion with gadolinium compound	PFOB or PFCE	MRI for evaluation and quantification of atherosclerotic lesions	^{19}F *In vitro, ex vivo* on an isolated hearts of pigs and *in vivo* on rabbits	(81,96)
Peptidomimetic nanoemulsion	PFCE	MR molecular imaging and detection of angiogenesis in sclerotic aortic valves	^{19}F spectroscopy and imaging of fibrin clots of an *ex vivo* human carotid arteries sample	(103)
Peptidomimetic nanoemulsion with gadolinium compound	PFOB	Characterization and MR molecular imaging of angiogenesis	*Ex vivo* ^{19}F spectroscopy and MRI on rabbits	(102)
Proteinic and pegylated microcapsules	PFN	MRI of mononuclear phagocyte system	MRI *in vivo* in tumor xenograft in mice.	(108)
Polymeric nanocapsules	PFOB	Blood pool contrast for hepatic imaging	*In vivo* MRI and biodistribution in rats	(65)
	PFCE	MRI contrast agent tissue-specific	*In vitro* MRI and MR Spectroscopy NMR characterization	(109)

substantial volumes of dissolved gases. Additionally, researchers observed that the MR relaxation times (T1) of liquid PFCs were sensitive to oxygen tension (pO$_2$) (85,86). Therefore, the ability to non-invasively monitor pO$_2$ *in vivo* using ^{19}F-MR has been investigated for oxygen imaging and quantitative determination of oxygenation of tissues concentrating PFCs, such as the lungs, the mononuclear phagocyte system, the heart and the brain, following intravenous or intraperitoneal administration (87–95). These studies have shown that tissue oxygenation could be measured successfully using commercial emulsions of either PFOB or perfluorotributylamine (PFTBA).

PFC Nanoemulsions

The group of Lanza and Wickline has studied the potential of nanoemulsions for ^{19}F MRI. Nanoemulsions of PFOB or perfluoro-15-crown-5-ether (PFCE) of ~250 nm were functionalized using biotinylated lipids for targeted MR molecular imaging. In order to obtain a dual contrast agent for both ^{1}H and ^{19}F MRI, lipidic gadolinium chelates, such as gadolinium-diethylene-triamine-pentaacetic acid bis-oleate (Gd-DTPA-BOA), were introduced in the formulation, also playing the role of emulsion stabilizers (Fig. 10) (81,96,97). PFC nanodroplets provide an enormous surface area to transport vast quantities of paramagnetical metal (~100,00 gadolinium ions per droplet) and thus concentrate it at different vascular sites. In addition to the surface payload of paramagnetic chelates, the liquid perfluorocarbon core represents 98% of the PFC droplet by volume, which equates for PFOB to a ^{19}F concentration of approximately 100 M within each droplet, sufficient to yield a good ^{19}F MRI signal (81).

The paramagnetic fluorinated nanoemulsions were first used for the detection, quantification and *in vivo* targeting of atherosclerosis lesions (96). As microdeposits of fibrin are the main indicators of artherosclerotic plaque, the detection and quantification of concentrations of fibrin in lesions was evaluated with functionalized nanoemulsions. The concentration of targeted nanoemulsions and hence fibrin epitopes was quantified based on the fluorine spectral signature with ^{19}F spectroscopy and MRI. Molecular binding was accomplished with the use of highly specific monoclonal antibody ligands and led to localization of MR signal amplification to the area of pathology with little competing blood pool signal. The detection of molecular binding was based on registration of the unique fluorine signal associated with these nanoemulsions contrast agents and the concentration of targeted nanoemulsions at high magnetic fields (96) but also at clinical magnetic field (81). Moreover, the pharmacokinetics profile and tissue distribution of targeted nanoemulsions were also evaluated by tracking the gadolinium associated to the surface of nanoemulsions in blood samples (98). The maximum amount of gadolinium that reached the targeted site was almost the double with targeted nanoemulsions than with non-targeted ones. By their specific binding and local accumulation, nanoemulsions demonstrated that the limited concentrations at the pathological site and the possible weakness of the fluorine signal as compared with proton can be overcome. Following these results, non-biotinylated nanoemulsions of PFCE were also used as contrast agent for angiography with cardiovascular magnetic resonance at clinical strength (99). The high level of signal
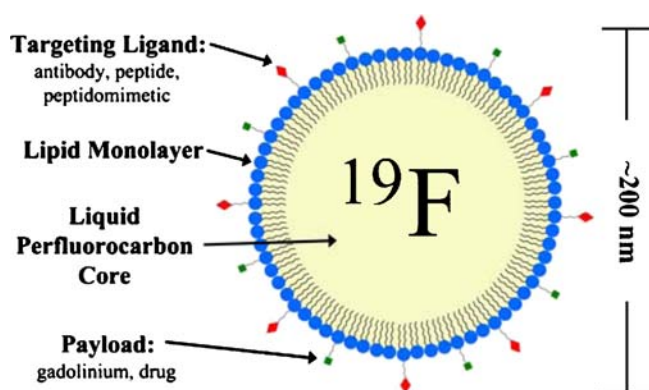
Fig. 10. Schematic representation of a multifunctional liquid perfluorocarbon nanoemulsion. The liquid perfluorocarbon core is surrounded by a lipid monolayer, which can be functionalized with targeting ligands and other payload (110). Reprinted with permission.

obtained for nanoemulsions on ^{19}F MR images allowed for applying this system for angiography of small vessels *in vitro*, *ex vivo* on pig hearts for detecting coronary vessels and *in vivo* on rabbits after injection into carotid arteries. Following the success obtained with paramagnetic fluorinated nanoemulsions in ^{19}F MRI, the same group has demonstrated their potential for different applications, such as tracking cells involved in pathological processes stem/progenitor cells (100,101), characterization and MR molecular imaging of angiogenesis in xenograft mouse with peptides (102) and specific detection of angiogenesis in a rabbit model of aortic valve disease (103).

Ahrens *et al.* (104) have developed perfluoro-15-crown-ether nanoemulsions of 100–200 nm and used them to label dendritic cells (DC) *ex vivo*. Since nanoemulsions did not modify DCs function, labelled DCs were injected *in vivo* to mice and successfully tracked after i.v. injection using ^{19}F-MRI at a magnetic field of 11.7 T (Fig. 11). The technique was then used to visualize and quantify the migration of diabetogenic T cells to the pancreas after injection to mice

using only ^{19}F-MRI (105) or combined with fluorescence detection (106).

Flögel *et al.* (107) developed a nanoemulsion of PFCE with a lipid mixture of lecithin and phosphatidylethanolamine for *in vivo* visualization of inflammatory processes in a murine model of acute cardiac and cerebral ischemia. Nanoemulsions of about 130 nm were also fluorescently labeled with rhodamine. An accumulation of ^{19}F-labeled cells within the injured areas was observed. ^{19}F MRI images enabled an exact anatomic localization of the liquid PFC after an i.v. injection and revealed a time-dependent infiltration of the injected nanoemulsions into the border zone of infarcted areas in both injury models (Fig. 12). Using rhodamine, circulating monocytes/macrophages were identified as the main cell fraction taking up injected nanoemulsions, providing a possibility for specifically labeling circulating monocytes/macrophages and following their fate within the body. Finally, nanoemulsions served as "positive" contrast agents for ^{19}F-MRI detection of inflammation, permitting a spatial resolution close to the anatomic ^{1}H image and an excellent degree of specificity resulting from the lack of any ^{19}F background.

PFC Microcapsules and Nanocapsules

Capsules of liquid PFC offer several advantages as compared to emulsions. First, because the encapsulation process is extremely efficient, the volume of PFC that can be delivered per unit injection volume is up to six times greater than for typical emulsion, increasing signal intensity and/or decreasing data adquisition time. Second, the surface reactive groups of capsule shell can be chemically modified to control their plasmatic half-life.

Using sonochemistry, Webb *et al.* (108) developed cross-linked bovine serum albumin shells encapsulating perfluorononane with a mean diameter of 2.5 µm. Microcapsule surface was alternatively PEGylated. Both types of microcapsules wer injected intravenously to rats. *In vivo* ^{19}F-MRI observations allowed for estimating the biodistribution on
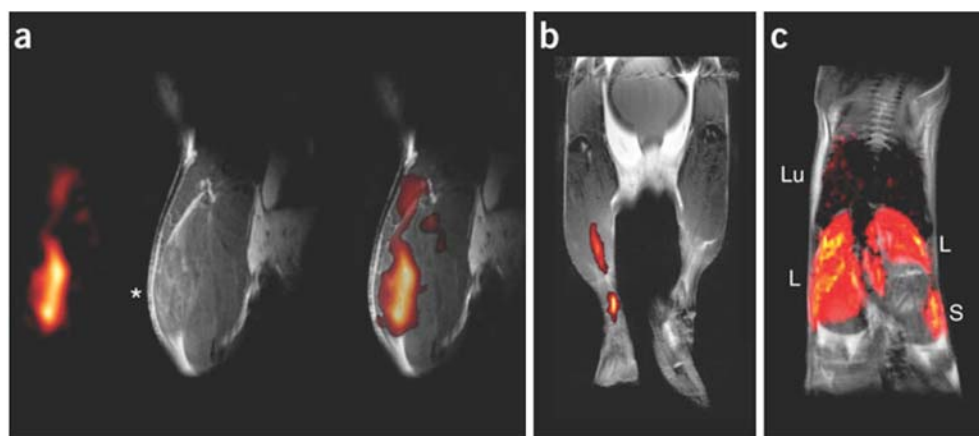

Fig. 11. *In vivo* MRI of PFPE-labeled dendritic cells (DCs) in mouse. The ^{19}F intensity is displayed on a "hot-iron" intensity scale, and the ^{1}H image is shown in gray scale. (**a**) Mouse quadriceps after intramuscular injection of PFPE-labeled DCs, asterisk indicates injection site. Shown (from left to right) are ^{19}F and ^{1}H images and a "composite" ^{19}F /^{1}H image. (**b**) Composite image of DC migration into the popliteal lymph node following a hind foot pad injection. (**c**) Composite image through the torso following i.v. inoculation with PFPE-labeled DCs. Cells are apparent in the liver (L), spleen (S) and weakly in the lungs (Lu) (104). Reprinted with permission.
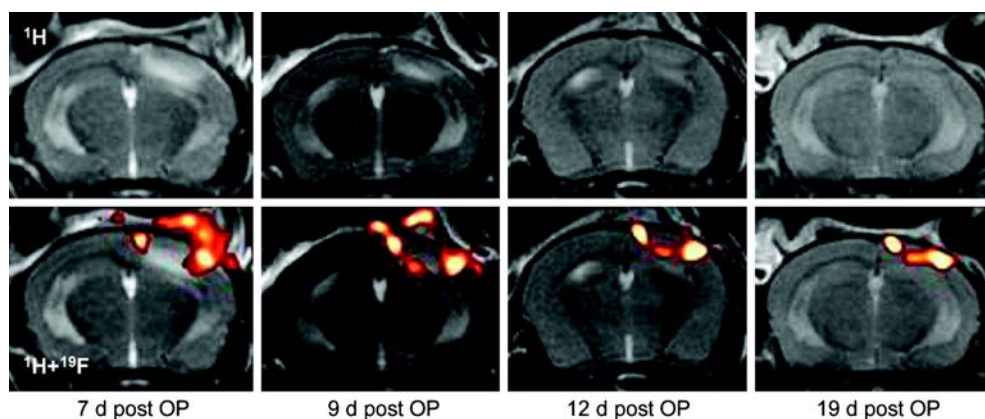
Fig. 12. Infiltration of PFCs into the brain after induction of focal cerebral ischemia by photothrombosis. Sections of brain ^{1}H images (*top*) from an individual mouse superimposed with the corresponding ^{19}F images (*red*, *bottom*) showing movement of the PFCs with the rim of the infarct over time. Initially, additional signal also was observed supracranial at the location of surgery. Images were obtained 7 days, 9 days, 12 days, and 19 days after induction of focal cerebral ischemia (post OP). PFCs were injected at day 0 (2 h after infarction) and day 6 via the tail vein (107). Reprinted with permission.

rats injected intravenously. The circulation half-life of PEGylated microcapsules was higher than unmodified microcapsules, 70 min *versus* 2.5 min, respectively. Passive targeting of the mononuclear phagocyte system by PEGylated microcapsules was used to specifically image the liver and the bone marrow. *In vivo,* high intensity was observed in the liver, whereas minor uptake by the bone marrow was evidenced.

Nyström *et al.* (109) described a method to create small nanocapsules (ca 20 nm) as MRI contrast agent encapsulating perfluoro-15-crown-5-ether (PFCE), a cyclic liquid PFC, within a shell of copolymers of styrene (PS) and 2,3,4,5,6-pentafluorostyrene (PPFS), as well as block copolymers with tert-butyl acrylate (PtBA)-b-PS-co-PPFS PEG-pentafluorostyrene. The shells of these nanocapsules derived from polymeric micelles assembled in aqueous solution have been crosslinked and their cores have been swollen with PFCE. It is worth mentioning that when encapsulated, PFCE was not detected in ^{19}F NMR. Hydrophobic fluorinated polymer chains present in the core most probably restricted the mobility of PFCE and prohibited any NMR signal from this molecule to be detected. Nanocapsules had to be further swollen with DMSO to increase PFCE mobility and recover PFCE ^{19}F NMR signal.

Recently, Pisani *et al.* (65) demonstrated that PFOB nanocapsules (64) could also be used as ^{19}F-MRI contrast agents. Neither the PFOB ^{19}F spectrum nor its characteristic relaxation times were modified by its encapsulation within the polymeric shell of PLGA. These results demonstrate that PFOB does not interact with PLGA, retains its mobility and is protected from molecules located outside the capsules. ^{19}F-MRI images of nanocapsules in suspension were easily obtained *in vitro* in up to 34 min (Fig. 13). These preliminary observations evidence the potentialities of these capsules as a dual-modality contrast agent since they are also efficient as UCAs.

CONCLUSIONS AND PERSPECTIVES

As compared with microbubbles, nano-systems encapsulating liquid PFC as UCAs are more stable under pressure and mechanical stress and are capable of carrying a larger drug payload. As a counterbalance, their echogenicity is weaker, in particular when particle size gets lower than 400 nm. Additionaly, since the intensity of acoustic scattering from spherical particles generally increases according to the sixth power of their radius, some form of particle aggregation
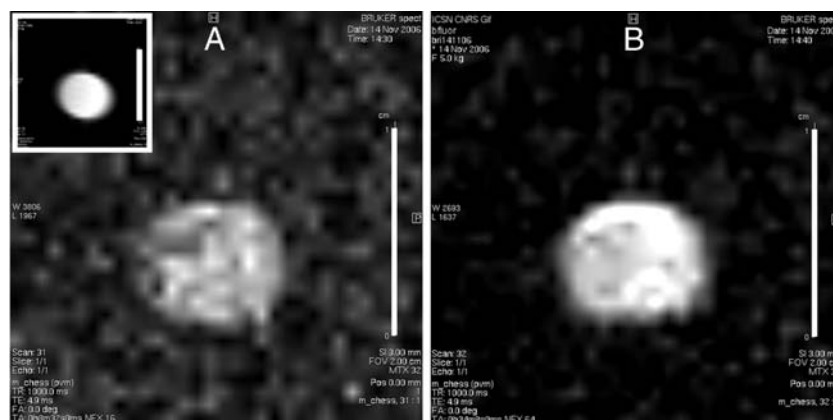

Fig. 13. 19 F MRI spin-echo images of pure PFOB (**A**, inset, 8 min) and 150 nm capsules suspended in water (50 mg ml^{-1}: **A**, 8 min; **B**, 34 min). Scale bars represent 1 cm (65). Reprinted with permission.

may provide an increased contrast. Interestingly, a marked enhancement of echogenicity has been observed when nano-systems were bound to a surface (51). PFC nano-systems exhibit low inherent echogenicity and poor blood contrast under conditions of conventional 2-D echocardiography or harmonic imaging, or when imaged with color flow or spectral Doppler (29). However, Wickline *et al*. (29) have shown that PFC nanoemulsions with a mean diameter around 400 nm can provide excellent blood pool contrast when imaged with Harmonic Power Doppler at dosage of 0.5 ml/kg (approximately 0.7% blood volume).

In addition to their potential for ultrasonography, liquid PFC nanoemulsions or nanocapsules have shown very promising results as contrast agents for ^{19}F-MRI, in combination with ^{1}H-MRI for anatomic imaging. Molecular imaging can even be considered due to the high sensitivity of ^{19}F-MRI using high magnetic field, provided MRI sequences are optimized.

In conclusion, ultrasonography and MRI are complementary. Both techniques are usually needed to discern possible pathological changes in tissue. If dual-modality contrast agents combining the advantages of the ultrasound and MR imaging could be applied clinically, adequate and comprehensive imaging information will be obtained using a single contrast agent. It would be convenient not only to medical professionals, but it would also reduce the healthcare costs. Emulsions and nano-systems encapsulating liquid PFC as contrast agent for ultrasonography and MRI have proven their potentialities for the imaging of blood pool, ventricular abnormalities, liver, thrombi, artherosclerosis, mononuclear phagocyte system, tumor, molecular imaging of angiogenesis and drug delivery carriers of anticancer drugs. The literature reviewed here provides enough indication to anticipate application of liquid PFC within nano-systems as potential dual contrast agents for ultrasonography and/or MRI for molecular and targeted imaging. Currently, research and development of contrast agents focuses mainly on tumor- or tissue-specific nano-systems, nanoemulsions and nanoparticules to detect, diagnose, treat and monitor therapy with the same product.

ACKNOWLEDGMENTS

REFERENCES

1. Riess JG. Blood substitutes and other potential biomedical applications of fluorinated colloids. J Fluorine Chem. 2002;114:119–26.
2. Gross U, Rudiger S, Reichelt H. Perfluorocarbons—chemically inert but biologically-active. J Fluorine Chem. 1991;53:155–61.
3. Lehmler HJ, Bummer PM, Jay M. Liquid ventilation—a new way to deliver drugs to diseased lungs? Chemtech. 1999;29:7–12.
4. Liuand MS, Long DM. Perfluoroctylbromide as a diagnostic contrast medium in gastroenterography. Radiology. 1977;122:71–6.
5. Lowe KC. Perfluorinated blood substitutes and artificial oxygen carriers. Blood Rev. 1999;13:171–84.
6. Leese PT, Noveck RJ, Shorr JS, Woods CM, Flaim KE, Keipert PE. Randomized safety studies of intravenous perflubron emulsion. I. Effects on coagulation function in healthy volunteers. Anesth Analg. 2000;91:804–11.
7. Noveck RJ, Shannon EJ, Leese PT, Shorr JS, Flaim KE, Keipert PE, *et al*. Randomized safety studies of intravenous perflubron emulsion. II. Effects on immune function in healthy volunteers. Anesth Analg. 2000;91:812–22.
8. Spahn DR. Blood substitutes artificial oxygen carriers: perfluorocarbon emulsions. Crit Care. 1999;3:R93–7.
9. Lowe KC. Engineering blood: synthetic substitutes from fluorinated compounds. Tissue Eng. 2003;9:389–99.
10. Gross GW, Greenspan JS, Fox WW, Rubenstein SD, Wolfson MR, Shaffer TH. Use of liquid ventilation with perflubron during extracorporeal membrane-oxygenation—chest radiographic appearances. Radiology. 1995;194:717–20.
11. Lozano JA, Castro JA, Rodrigo I. Partial liquid ventilation with perfluorocarbons for treatment of ARDS in burns. Burns. 2001;27:635–42.
12. Hamon I. Liquid ventilation: a new mode of ventilation in neonatology? Arch Pediatr. 1997;4:176–80.
13. Mattrey RF, Long DM, Multer F, Mitten R, Higgins CB. Perfluoroctylbromide: a reticuloendothelial-specific and tumor-imaging agent for computed tomography. Radiology. 1982;145:755–8.
14. Young SW, Enzmann DR, Long DM, Muller HH. Perfluoroctyl-bromide contrast enhancement of malignant neoplasms: preliminary observations. AJR Am J Roentgenol. 1981;137:141–6.
15. Klibanov AL. Ultrasound molecular imaging with targeted microbubble contrast agents. J Nucl Cardiol. 2007;14:876–84.
16. Mattrey RF. The potential role of perfluorochemicals (PFCs) in diagnostic imaging. Artif Cells Blood Substit Immobil Biotechnol. 1994;22:295–313.
17. Schutt EG, Klein DH, Mattrey RM, Riess JG. Injectable microbubbles as contrast agents for diagnostic ultrasound imaging: the key role of perfluorochemicals. Angew Chem Int Edit. 2003;42:3218–35.
18. Liu Y, Miyoshi H, Nakamura M. Encapsulated ultrasound microbubbles: therapeutic application in drug/gene delivery. J Control Release. 2006;114:89–99.
19. Dijkmans PA, Juffermans LJ, Musters RJ, van Wamel A, ten Cate FJ, van Gilst W, *et al*. Microbubbles and ultrasound: from diagnosis to therapy. Eur J Echocardiogr. 2004;5:245–56.
20. Lanzaand GM, Wickline SA. Targeted ultrasonic contrast agents for molecular imaging and therapy. Curr Probl Cardiol. 2003;28:625–53.
21. Hernotand S, Klibanov AL. Microbubbles in ultrasound-triggered drug and gene delivery. Adv Drug Deliv Rev. 2008;60:1153–66.
22. Oeffinger BE, Wheatley MA. Development and characterization of a nano-scale contrast agent. Ultrasonics. 2004;42:343–7.
23. Sontum PC. Physicochemical characteristics of Sonazoid (TM), a new contrast agent for ultrasound imaging. Ultrasound Med Biol. 2008;34:824–33.
24. Goldberg B. Ultrasound contrast agents. London: Dunitz; 2001.
25. Lindner JR. Microbubbles in medical imaging: current applications and future directions. Nat Rev Drug Discov. 2004;3:527–33.
26. Calliada F, Campani R, Bottinelli O, Bozzini A, Sommaruga MG. Ultrasound contrast agents: basic principles. Eur J Radiol. 1998;27(Suppl 2):S157–60.
27. Grant EG. Sonographic contrast agents in vascular imaging. Seminars in Ultrasound Ct and Mri. 2001;22:25–41.
28. Ngo FC, Hall CS, Marsh JN, Fuhrhop RW, Allen JS, *et al*. Evaluation of liquid perfluorocarbon nanoparticles as a blood pool contrast agent utilizing power Doppler harmonic imaging. 2000 Ieee Ultrasonics Symposium Proceedings. 2000;1 and 2:1931–4.
29. Wickline SA, Hughes M, Ngo FC, Hall CS, Marsh JN, Brown PA, *et al*. Blood contrast enhancement with a novel, non-gaseous nanoparticle contrast agent. Acad Radiol. 2002;9:S290–3.
30. Bokor D. Diagnostic efficacy of SonoVue. Am J Cardiol. 2000;86:19G–24.
31. Kitzman DW, Goldman ME, Gillam LD, Cohen JL, Aurigemma GP, Gottdiener JS. Efficacy and safety of the novel ultrasound contrast agent perflutren (definity) in patients with suboptimal baseline left ventricular echocardiographic images. Am J Cardiol. 2000;86:669–74.

32. Lindner JR, Song J, Jayaweera AR, Sklenar J, Kaul S. Microvascular rheology of Definity microbubbles after intra-arterial and intravenous administration. J Am Soc Echocardiogr. 2002;15:396–403.

33. Cohen JL, Cheirif J, Segar DS, Gillam LD, Gottdiener JS, Hausnerova E, et al. Improved left ventricular endocardial border delineation and opacification with OPTISON (FS069), a new echocardiographic contrast agent. Results of a phase III Multicenter Trial. J Am Coll Cardiol. 1998;32:746–52.

34. Correas JM, Bridal L, Lesavre A, Mejean A, Claudon M, Helenon O. Ultrasound contrast agents: properties, principles of action, tolerance, and artifacts. Eur Radiol. 2001;11:1316–28.

35. Straub JA, Chickering DE, Church CC, Shah B, Hanlon T, Bernstein H. Porous PLGA microparticles: AI-700, an intravenously administered ultrasound contrast agent for use in echocardiography. J Control Release. 2005;108:21–32.

36. Cui W, Bei J, Wang S, Zhi G, Zhao Y, Zhou X, et al. Preparation and evaluation of poly(L-lactide-co-glycolide) (PLGA) microbubbles as a contrast agent for myocardial contrast echocardiography. J Biomed Mater Res B Appl Biomater. 2005;73:171–8.

37. El-Sherif DM, Wheatley MA. Development of a novel method for synthesis of a polymeric ultrasound contrast agent. J Biomed Mater Res A. 2003;66:347–55.

38. Quay S. Microbubble-based ultrasound contrast agents: the role of gas selection in microbubble persistence. J Ultrasound Med. 1994;13:S9.

39. Mattrey RF, Scheible FW, Gosink BB, Leopold GR, Long DM, Higgins CB. Perfluoroctylbromide: a liver/spleen-specific and tumor-imaging ultrasound contrast material. Radiology. 1982;145:759–62.

40. Ragde H, Kenny GM, Murphy GP, Landin K. Transrectal ultrasound microbubble contrast angiography of the prostate. Prostate. 1997;32:279–83.

41. Ge S, Giraud GG, Shiota T, Pantely GA, Xu J, Gong Z, et al. Microcirculatory flow dynamics during peripheral intravenous injection of echogentm: microscopic visualization of mesenteric microcirculatory flow with simultaneous transthoracic echo imaging in cats. J Am Coll Cardiol. 1995;25:227A.

42. Cotter B, Duong A, Raisinghani A, Keramati S, Mahmud E, Kwan OL, et al. Myocardial opacification by low doses EchoGen in patients: assessment of preactivation by closed syringe suction. J Am Coll Cardiol. 1996;27:126.

43. Nihoyannopoulos P, Rallidis L, Correas J-M, Quay SC. Myocardial enhancement following peripheral intravenous injection of activated QW3600 (EchoGen) in normal human volunteers. J Am Coll Cardiol. 1996;27:378.

44. Grayburn P. Perflenapent emulsion (EchoGen): a new long-acting phase-shift agent for contrast echocardiography. Clin Cardiol. 1997;20:I12–8.

45. Kornmann LM, Curfs DMJ, Hermeling E, van der Made I, de Winther MPJ, Reneman RS, et al. Perfluorohexane-loaded macrophages as a novel ultrasound contrast agent: a feasibility study. Mol Imaging Biol. 2008;10:264–70.

46. Saha P, Modarai B, Humphries J, Mattock K, Waltham M, Burnand KG, et al. The monocyte/macrophage as a therapeutic target in atherosclerosis. Curr Opin Pharmacol. 2009;9:109–18.

47. Gref R, Minamitake Y, Peracchia MT, Trubetskoy V, Torchilin V, Langer R. Biodegradable long-circulating polymeric nanospheres. Science. 1994;263:1600–3.

48. Yuan F, Dellian M, Fukumura D, Leunig M, Berk DA, Torchilin VP, et al. Vascular permeability in a human tumor xenograft: molecular size dependence and cutoff size. Cancer Res. 1995;55:3752–6.

49. Gref R, Luck M, Quellec P, Marchand M, Dellacherie E, Harnisch S, et al. 'Stealth' corona-core nanoparticles surface modified by polyethylene glycol (PEG): influences of the corona (PEG chain length and surface density) and of the core composition on phagocytic uptake and plasma protein adsorption. Colloids Surf B Biointerfaces. 2000;18:301–13.

50. Pasqualini R, Arap W, McDonald DM. Probing the structural and molecular diversity of tumor vasculature. Trends Mol Med. 2002;8:563–71.

51. Lanza GM, Wallace KD, Scott MJ, Cacheris WP, Abendschein DR, Christy DH, et al. A novel site-targeted ultrasonic contrast agent with broad biomedical application. Circulation. 1996;94:3334–40.

52. Lanza GM, Abendschein DR, Hall CS, Scott MJ, Scherrer DE, Houseman A, et al. In vivo molecular imaging of stretch-induced tissue factor in carotid arteries with ligand-targeted nanoparticles. J Am Soc Echocardiogr. 2000;13:608–14.

53. Winslow RM. Blood substitutes. Adv Drug Deliv Rev. 2000;40:131–42.

54. Hall CS, Marsh JN, Scott MJ, Gaffney PJ, Wickline SA, Lanza GM. Temperature dependence of ultrasonic enhancement with a site-targeted contrast agent. J Acoust Soc Am. 2001;110:1677–84.

55. Marsh JN, Hall CS, Wickline SA, Lanza GM. Temperature dependence of acoustic impedance for specific fluorocarbon liquids. J Acoust Soc Am. 2002;112:2858–62.

56. Marsh JN, Hall CS, Scott MJ, Fuhrhop RW, Gaffney PJ, Wickline SA, et al. Improvements in the ultrasonic contrast of targeted perfluorocarbon nanoparticles using an acoustic transmission line model. IEEE Trans Ultrason Ferroelectr Freq Control. 2002;49:29–38.

57. Marsh JN, Partlow KC, Abendschein DR, Scott MJ, Lanza GM, Wickline SA. Molecular imaging with targeted perfluorocarbon nanoparticles: quantification of the concentration dependence of contrast enhancement for binding to sparse cellular epitopes. Ultrasound Med Biol. 2007;33:950–8.

58. Hughes MS, Marsh JN, Zhang H, Woodson AK, Allen JS, Lacy EK, et al. Characterization of digital waveforms using thermodynamic analogs: Detection of contrast-targeted tissue in vivo. IEEE Trans Ultrason Ferroelectr Freq Control. 2006;53:1609–16.

59. Hughes MS, McCarthy JE, Marsh JN, Arbeit JM, Neumann RG, Fuhrhop RW, et al. Properties of an entropy-based signal receiver with an application to ultrasonic molecular imaging. J Acoust Soc Am. 2007;121:3542–57.

60. Hughes MS, Marsh JN, Arbeit JM, Neumann RG, Fuhrhop RW, Wallace KD, et al. Application of Renyi entropy for ultrasonic molecular imaging. J Acoust Soc Am. 2009;125:3141–5.

61. Couture O, Bevan PD, Cherin E, Cheung K, Burns PN, Foster FS. Investigating perfluorohexane particles with high-frequency ultrasound. Ultrasound Med Biol. 2006;32:73–82.

62. Couture O, Bevan PD, Cherin E, Cheung K, Burns PN, Foster FS. A model for reflectivity enhancement due to surface bound submicrometer particles. Ultrasound Med Biol. 2006;32:1247–55.

63. El-Sherif DM, Lathia JD, Le NT, Wheatley MA. Ultrasound degradation of novel polymer contrast agents. J Biomed Mater Res A. 2004;68:71–8.

64. Pisani E, Tsapis N, Paris J, Nicolas V, Cattel L, Fattal E. Polymeric nano/microcapsules of liquid perfluorocarbons for ultrasonic imaging: physical characterization. Langmuir. 2006;22:4397–402.

65. Pisani E, Tsapis N, Galaz B, Santin M, Berti R, Taulier N, et al. Perfluorooctyl bromide polymeric capsules as dual contrast agents for ultrasonography and magnetic resonance imaging. Adv Funct Mater. 2008;18:2963–71.

66. Pisani E, Fattal E, Paris J, Ringard C, Rosilio V, Tsapis N. Surfactant dependent morphology of polymeric capsules of perfluorooctyl bromide: Influence of polymer adsorption at the dichloromethane-water interface. J Colloid Interface Sci. 2008;326:66–71.

67. Reed AM, Gilding DK. Biodegradable polymers for use in surgery—poly(glycolic)/poly(lactic acid) homo and copolymers: 2. In vitro degradation. Polymer. 1981;22:494–8.

68. Yamaguchiand K, Anderson JM. Invivo biocompatibility studies of medisorb(R) 65/35 D. L-lactide glycolide copolymer microspheres. J Control Release. 1993;24:81–93.

69. Owens DE 3rd, Peppas NA. Opsonization, biodistribution, and pharmacokinetics of polymeric nanoparticles. Int J Pharm. 2006;307:93–102.

70. Harris JM, Chess RB. Effect of pegylation on pharmaceuticals. Nat Rev Drug Discov. 2003;2:214–21.

71. Diaz-Lopez R, Tsapis N, Libong D, Chaminade P, Connan C, Chehimi MM, et al. Phospholipid decoration of microcapsules containing perfluorooctyl bromide used as ultrasound contrast agents. Biomaterials. 2009;30:1462–72.

72. Fang JY, Hung CF, Hua SC, Hwang TL. Acoustically active perfluorocarbon nanoemulsions as drug delivery carriers for camptothecin: drug release and cytotoxicity against cancer cells. Ultrasonics. 2009;49:39–46.

73. Rapoport N, Gao Z, Kennedy A. Multifunctional nanoparticles for combining ultrasonic tumor imaging and targeted chemotherapy. J Natl Cancer Inst. 2007;99:1095–106.

74. Gao Z, Kennedy AM, Christensen DA, Rapoport NY. Drug-loaded nano/microbubbles for combining ultrasonography and targeted chemotherapy. Ultrasonics. 2008;48:260–70.

75. Maeda H. The enhanced permeability and Retention (EPR) effect in tumor vasculature: the key role of tumor-selective macro-molecular drug targeting. Advan Enzyme Regul. 2001;41:189–207.

76. Uchegbu I. Parenteral drug delivery: 1. Pharm J. 1999;263:309–18.

77. Waters EA, Wickline SA. Contrast agents for MRI. Basic Res Cardiol. 2008;103:114–21.

78. McKieand S, Brittenden J. (ii) Basic science: magnetic resonance imaging. Curr Orthop. 2005;19:13–9.

79. Yan G-P, Robinson L, Hogg P. Magnetic resonance imaging contrast agents: overview and perspectives. Radiography. 2007;13:e5–19.

80. Hengererand A, Grimm J. Molecular magnetic resonance imaging. Biomed Imaging Intervention J. 2006;2:e8.

81. Caruthers SD, Neubauer AM, Hockett FD, Lamerichs R, Winter PM, Scott MJ, et al. In vitro demonstration using F-19 magnetic resonance to augment molecular imaging with paramagnetic perfluorocarbon nanoparticles at 1.5 Tesla. Invest Radiol. 2006;41:305–12.

82. Holland GN, Bottomley PA, Hinshaw WS. 19F magnetic resonance imaging. J Magn Reson. 1977;28:133–6.

83. Kimura A, Narazaki M, Kanazawa Y, Fujiwara H. 19F Magnetic resonance imaging of perfluorooctanoic acid encapsulated in liposome for biodistribution measurement. Magn Reson Imaging. 2004;22:855–60.

84. Schwarz R, Schuurmans M, Seelig J, Kunnecke B. 19F-MRI of perfluorononane as a novel contrast modality for gastrointestinal imaging. Magn Reson Med. 1999;41:80–6.

85. Mason RP, Nunnally RL, Antich PP. Tissue oxygenation: a novel determination using 19F surface coil NMR spectroscopy of sequestered perfluorocarbon emulsion. Magn Reson Med. 1991;18:71–9.

86. Clark LC Jr, Ackerman JL, Thomas SR, Millard RW, Hoffman RE, Pratt RG, et al. Perfluorinated organic liquids and emulsions as biocompatible NMR imaging agents for 19F and dissolved oxygen. Adv Exp Med Biol. 1984;180:835–45.

87. Mason RP, Shukla H, Antich PP. Oxygent(Tm)—a novel probe of tissue oxygen-tension. Biomaterials Artificial Cells and Immobilization Biotechnology. 1992;20:929–32.

88. Mason RP, Shukla H, Antich PP. In vivo oxygen-tension and temperature—simultaneous determination using f-19 nmr-spectroscopy of perfluorocarbon. Magn Reson Med. 1993;29:296–302.

89. Shukla HP, Mason RP, Storey C, Jeffrey FMH, Antich PP. The relationship of oxygen-tension and myocardial mechanical function—a F-19 Nmr-study. Circulation. 1992;86:693–3.

90. Shukla HP, Mason RP, Bansal N, Antich PP. Regional myocardial oxygen tension: F-19 MRI of sequestered perfluorocarbon. Magn Reson Med. 1996;35:827–33.

91. Shukla HP, Mason RP, Woessner DE, Antich PP. Comparison of 3 commercial perfluorocarbon emulsions as high-field F-19 Nmr probes of oxygen-tension and temperature. J Magn Reson B. 1995;106:131–41.

92. Thomas SR, Pratt RG, Millard RW, Samaratunga RC, Shiferaw Y, McGoron AJ, et al. In vivo PO2 imaging in the porcine model with perfluorocarbon F-19 NMR at low field. Magn Reson Imaging. 1996;14:103–14.

93. Mason RP. Non-invasive physiology: 19F NMR of perfluorocarbons. Artif Cells Blood Substit Immobil Biotechnol. 1994;22:1141–53.

94. Eidelberg D, Johnson G, Barnes D, Tofts PS, Delpy D, Plummer D, et al. 19F NMR imaging of blood oxygenation in the brain. Magn Reson Med. 1988;6:344–52.

95. Fishman JE, Joseph PM, Floyd TF, Mukherji B, Sloviter HA. Oxygen-sensitive 19F NMR imaging of the vascular system in vivo. Magn Reson Imaging. 1987;5:279–85.

96. Morawski AM, Winter PM, Yu X, Fuhrhop RW, Scott MJ, Hockett F, et al. Quantitative "magnetic resonance immunohistochemistry" with ligand-targeted (19)F nanoparticles. Magn Reson Med. 2004;52:1255–62.

97. Winter P, Athey P, Kiefer G, Gulyas G, Frank K, Fuhrhop R, et al. Improved paramagnetic chelate for molecular imaging with MRI. Proceedings of the Fifth International Conference on Scientific and Clinical Apllications of Magnetic Carriers. J Magn Magn Mater. 2005;293:540–5.

98. Neubauer AM, Sim H, Winter PM, Caruthers SD, Williams TA, Robertson JD, et al. Nanoparticle pharmacokinetic profiling in vivo using magnetic resonance imaging. Magn Reson Med. 2008;60:1353–61.

99. Neubauer AM, Caruthers SD, Hockett FD, Cyrus T, Robertson JD, Allen JS, et al. Fluorine cardiovascular magnetic resonance angiography in vivo at 1.5 T with perfluorocarbon nanoparticle contrast agents. J Cardiovasc Magn Reson. 2007;9:565–73.

100. Partlow KC, Chen J, Brant JA, Neubauer AM, Meyerrose TE, Creer MH, et al. 19F magnetic resonance imaging for stem/progenitor cell tracking with multiple unique perfluorocarbon nanobeacons. Faseb J. 2007;21:1647–54.

101. Ruiz-Cabello J, Walczak P, Kedziorek DA, Chacko VP, Schmieder AH, Wickline SA, et al. In vivo "hot spot" MR imaging of neural stem cells using fluorinated nanoparticles. Magn Reson Med. 2008;60:1506–11.

102. Schmieder AH, Caruthers SD, Zhang H, Williams TA, Robertson JD, Wickline SA, et al. Three-dimensional MR mapping of angiogenesis with alpha5beta1(alpha nu beta3)-targeted theranostic nanoparticles in the MDA-MB-435 xenograft mouse model. Faseb J. 2008;22:4179–89.

103. Waters EA, Chen J, Allen JS, Zhang H, Lanza GM, Wickline SA. Detection and quantification of angiogenesis in experimental valve disease with integrin-targeted nanoparticles and 19-fluorine MRI/MRS. J Cardiovasc Magn Reson. 2008;10:43.

104. Ahrens ET, Flores R, Xu HY, Morel PA. In vivo imaging platform for tracking immunotherapeutic cells. Nat Biotechnol. 2005;23:983–7.

105. Srinivas M, Morel PA, Ernst LA, Laidlaw DH, Ahrens ET. Fluorine-19 MRI for visualization and quantification of cell migration in a diabetes model. Magn Reson Med. 2007;58:725–34.

106. Janjic JM, Srinivas M, Kadayakkara DKK, Ahrens ET. Self-delivering nanoemulsions for dual fluorine-19 MRI and fluorescence detection. J Am Chem Soc. 2008;130:2832–41.

107. Flogel U, Ding Z, Hardung H, Jander S, Reichmann G, Jacoby C, et al. In vivo monitoring of inflammation after cardiac and cerebral ischemia by fluorine magnetic resonance imaging. Circulation. 2008;118:140–8.

108. Webb AG, Wong M, Kolbeck KJ, Magin R, Suslick KS. Sonochemically produced fluorocarbon microspheres: a new class of magnetic resonance imaging agent. J Magn Reson Imaging. 1996;6:675–83.

109. Nystrom AM, Bartels JW, Du W, Wooley KL. Perfluorocarbon-loaded shell crosslinked knedel-like nanoparticles: lessons regarding polymer mobility and self-assembly. J Polym Sci A-Polym Chem. 2009;47:1023–37.

110. Kaneda MM, Caruthers S, Lanza GM, Wickline SA. Perfluorocarbon nanoemulsions for quantitative molecular imaging and targeted therapeutics. Ann Biomed Eng. 2009.